SCIENTIFIC PAPER
Published: November 6, 2024
https://doi.org/10.13167/2024.29.7

Development of single and multi-coil MR damper subjected to cyclic loading for structural vibration control

Daniel Cruze[1], Nedunchezhian Krishnaraju[1] and Balaji Ramalingam[1]

[1] Hindustan Institute of Technology and Science, Department of Civil Engineering, 603103, Chennai, Tamil Nadu, India

Corresponding author:
Daniel Cruze
danielckarunya@gmail.com

Received:
March 6, 2024

Revised:
March 27, 2024

Accepted:
April 17, 2024

Published:
November 6, 2024

Citation:
Cruze, D.; Krishnaraju, N.; Ramalingam, B. Development of single and multi-coil MR damper subjected to cyclic loading for structural vibration control. *Advances in Civil and Architectural Engineering,* 2024, 15 (29), pp. 106-119. https://doi.org/10.13167/2024.29.7

ADVANCES IN CIVIL AND ARCHITECTURAL ENGINEERING (ISSN 2975-3848)

Faculty of Civil Engineering and Architecture Osijek
Josip Juraj Strossmayer University of Osijek
Vladimira Preloga 3
31000 Osijek
CROATIA

Abstract:
The magnetorheological (MR) damper can dissipate energy from a vibrating system with low power consumption, making it one of the most popular semi-active damping devices. This study compares single- and multi-coil dampers subjected to cyclic loading. A magnetic oil-based MR fluid is synthesized with 50% carbonyl iron and 50 % synthetic oil, resulting in maximum damping force and minimum sedimentation. A three-dimensional model of the MR damper is created using AutoCAD and is fabricated. Single- and multi-coil MR dampers with a 3000 N capacity are designed and fabricated. The MR dampers are experimentally tested in a universal testing machine with a 1000 kN capacity for various input currents from 1 to 3 A. As the current increases, the damping force also increases in both the single- and multi-coil MR dampers. The multi-coil MR damper has a maximum damping force of 2628 N at a 15 mm amplitude, and the single-coil MR damper has a maximum damping force of 1868 N. A numerical simulation of the magnetic properties of the single- and multi-coil MR dampers is conducted using the finite-element method magnetics. A spring is placed at the top of the piston pole and bottom of the piston to make the MR damper semi-active. The fabricated MR damper can be used in seismic-resistant structures and as a base isolator to protect the structure from vibrations. In addition to civil engineering, it can be used in the development of adaptive prosthetics and orthotic devices, providing dynamic support.

Keywords:
MR damper; semi-active damper; single coil; multi-coil; MR fluid

1 Introduction

In recent years, the development of control systems for structures and infrastructures to monitor and minimise the effects of earthquake vibrations has become a significant area of research and technological advancement. These control systems are designed to enhance the resilience of structures and mitigate the damage caused by seismic events. A magnetorheological (MR) damper can dissipate energy from a vibrating system with a low power consumption, making the MR damper one of the most popular semi-active damping devices.

Cruze et al. [1] applied a semi-active control approach to a three-storey model structure using shear-mode MR dampers. Force–time results were obtained from experimental investigations using the MR damper. Response control was achieved using a small control force, with 2 A. The MR-damper position played a crucial role in the effectiveness of the response control. An MR damper incorporated into a smart semi-active control strategy was fabricated. The scaled-down single-story RC frame exhibited a 90 % average reduction in lateral displacement during four seismic events. As an economical and intelligent choice, the device enhances seismic resilience in earthquake-prone regions [2]. The MR damper was analysed using various finite-element-method software programs and its performance was experimentally evaluated. The proposed MR damper generated a force of 750 N with a 0,6 A current. It effectively reduced vibrations in both active and semi-active control systems [3]. The MR damper underwent assessment in a damping-force testing machine covering a range of excitation frequencies and supplied currents. Desai et al. conducted experiments for varying current levels (0-1,50 A in 0,25 A increments) applied to the MR damper. Force-displacement analyses revealed an increase in the damping force with increased velocity and current supplied to the MR damper [4]. The damper force in the MR damper is directly affected by the input-command voltage. Higher input voltages generally result in a greater damping force. Kori et al. conducted a parametric study in which the input command voltage of MR dampers was varied within the range of 0-10 V [5].

Olivier et al. [6] designed an MR damper with a unique combination of an electromagnet and two permanent magnets. The proposed model has the additional advantage of providing a moderate damping force in the case of electromagnetic failure. The results of the optimised parameters revealed that the damping force varied from 1383 N at a current of 0 A to 4141 N at a current of 2,0 A. The damping force was improved by more than 165 % compared with a previous model of the same size. In this study, the performance of the MR damper was compared under three different conditions: with the MR damper at a current of 0 A, with the MR damper at a current of 3 A, and without the MR damper. The MR damper under investigation demonstrated a significantly higher damping force when it had an electrical current of 3 A compared to when it had no current (0 A). The damping force increased by approximately 700 N for each 0,5 A increment [7]. Wang et al. compared the magnetorheological bifold valve (MRBV) and magnetorheological annular valve (MRAV) dampers for base-excited vibration isolation in the same external volume. The MRBV, with a 31,6 ml MR fluid volume (73 % less than the 115,08 ml of the MRAV), exhibited a superior dynamic range (1-15 Hz) and improved skyhook control performance in a single degree-of-freedom vibration-control system, highlighting its potential for efficient and cost-effective base-excited vibration isolation [8]. Their study revealed that the temperature levels increased with a higher input voltage and frequency of excitation. This indicates a direct correlation between the temperature and operational parameters of the MR damper. The dampers were tested for 0 A, 0,25 A, 0,50 A, and 1,00 A at frequencies of 0,5; 1,0; 1,5; 2,0 and 3,0 Hz for each current value. At each displacement, amplitudes of 5, 10, and 15 mm for the short-stroke damper and 5, 10, 15, and 20 mm for the long-stroke damper were provided, and the values were recorded for ten cycles [9]. Jovar et al. aimed to mitigate the earthquake response through the implementation of an MR damping system in a three-span bridge. The three-span bridge (12 m in length) was modelled with MR dampers connecting each span. The MR damping system,

when applied with control algorithms, demonstrated a 35 % maximum reduction and 10 % minimum reduction [10].
Research on MR dampers has emphasised flow- and shear-mode types. Finite-element-method magnetic (FEMM) software was used for optimisation. The damping force with 586 turns and 1 A current in the squeeze-mode damper was close to 4222 N [11].
Yazid et al. [12] introduced a new concept for an MR damper that incorporated both shear and squeeze working modes. FEMM was employed to simulate the magnetic field generated by the electromagnetic coils in the MR damper. Increasing applied current led to an increase in force, reaching up to 100 N with 0,4 A in shear mode. Near the end-wall position (50 mm distance), with the piston nearing the bottom, the squeeze force significantly increased up to 250 N with 0,4 A in squeeze mode. The main objective was to compare a parametric model with experimental data to choose the appropriate parameters for the modified Bouc–Wen model, which was chosen to mathematically describe the behaviour of MR dampers. The comparison involved studying the force–velocity and force–displacement relationships. The small values in the percentage difference for force (0,5-3,5%) indicate the accuracy of the modified Bouc–Wen model in portraying the characteristics and behaviour of the MR damper [13]. Aggümüş et al. [14] investigated the efficacy of a semi-active tuned mass damper (STMD) in mitigating building vibrations during seismic events using real-time hybrid simulation (RTHS). The dynamic and adaptive ground-hook control algorithm determined MR-damper voltage based on the ground motion. These results suggested that RTHS is a viable alternative to traditional experiments for evaluating STMD performance in structural vibration control. Fu et al. [15] presented a structural vibration-control system that incorporated base isolation with rubber bearings and MR dampers to overcome the limitations of conventional methods. Shaking-table tests were used to evaluate the system performance under various earthquake conditions. Rubber bearings provided a restoring force, satisfied deformation constraints, particularly in infrequent earthquakes, enhanced structural resilience and seismic performance, and addressed the shortcomings of traditional methods. Six MR fluids were prepared by varying carbonyl iron (CI) particle percentages and carrier liquids. The rheological analysis, notably that of MRF 80, showed superior performance to that of commercial MRF 132 DG. Damper experiments concentrated on MRF 80 with a 1-mm annular gap and demonstrated a peak damping force of 536 N in cyclic load tests [16]. The main focus of this study was on how the MR fluid performs differently following prolonged cyclic stress in a fatigue dynamic machine. In both the on and off modes, the MR damper's damping force increased. After 170,000 operational cycles, specific increases of 44 % in the on-state condition and 90% in the off-state condition were observed [17]. Magnetorheological fluids (MRFs) are promising for impact mitigation with controllable rheological properties under magnetic fields. Rheological examination using a speed-controlled capillary magnetorheometer revealed consistent shear-thinning behaviour. Viscosity correlated directly with magnetic-field strength, demonstrating uniformity across diverse excitation levels [18]. Harsh et al. developed MRF using paraffin oil, CI particles, and grease. The proportion of CI particles and the addition of grease significantly influenced the sedimentation ratio of the MRF. The yield stress was observed to increase with a higher proportion of CI particles and the introduction of a magnetic field [19]. Shake-table tests were conducted to evaluate the performance of the shear-mode MR damper. The results demonstrated a substantial reduction in displacement ranging from 40 to 67 %. This indicates the effectiveness of the MR damper in reducing vibrations induced by seismic forces. In terms of flow rate, the one-stage model with a 1,6 A current exhibited the largest pressure reduction [20]. This study presented the conceptual design, fabrication, and experimental characterisation of a mid-sized, large-capacity MR damper equipped with a compact annular-radial MR-fluid bypass valve, demonstrating the advancements in MR-damper design and engineering. The bypass configuration of the MR damper enabled modifications to the MR-valve design, resulting in considerably higher dynamic indices, including a maximum dynamic range of 5,06 and maximum damping force of 6,61 kN, highlighting the potential for enhanced performance through design optimisation [21]. Devikiran et al. [22] demonstrated the improved performance of an MR damper in mitigating road disturbances when equipped with a

proportional-integral-derivative (PID) controller, highlighting the effectiveness of active control strategies in enhancing ride comfort and handling stability. A PID control system was designed to effectively regulate the MR damper based on its deflection, enhancing its adaptability to varying road conditions. Despite its improved performance, the MR damper maintained a maximum power consumption of 18 W [22]. The Non-dominated Sorting Genetic Algorithm version II was utilised in this study to optimise the structure of MR dampers, aiming to enhance their performance. The design principles of the MR damper were described, including the selection of the magnetic-circuit materials and MR fluids that were crucial for achieving the desired performance characteristics. The maximum output of the damper was recorded at 1774,1 N, which significantly exceeded the force of 150,35 N [23]. Zhang et al. [24] explored three types of MRDs: internal, bypass, and hybrid, focusing on their structural design and engineering applications. Internal MRDs emphasised the rationalisation of coil numbers and arrangements, optimisation of piston structures, and extension of damping-channel lengths. Bypass MRDs optimised geometric arrangements, offering a wide dynamic-adjustment range, but encountered space challenges. Hybrid MRDs blended internal and bypass structures, enhancing the overall performance by mitigating single-mode disadvantages and satisfying diverse damping requirements. These advancements have paved the way for improved MRD designs with enhanced magnetic-field utilisation across various industries. Tharehalli et al. [25] focused on evaluating the dynamic performance of a semiactive quarter-car vehicle under random road conditions. The modelled MR damper served as a variable damper within a semi-active suspension system. By adjusting the damping characteristics in real time, the system aimed to optimise vehicle dynamics and passenger comfort. The SMC provided better controllability than a PID controller, particularly under challenging road conditions. This underscores the effectiveness of the SMC approach in improving the vehicle dynamics and passenger comfort.

In this study, single- and multi-coil MR dampers subjected to cyclic loading are compared. The main focus of this project is to comprehensively analyse single- and multi-coil MR dampers. The study begins with a meticulous three-dimensional (3D) modelling of the MR damper, considering the arrangement and dimensions of the coils for both single- and multi-coil setups. The next step is the fabrication process, in which the 3D models are transformed into physical prototypes with strict adherence to the design specifications and rigorous quality-control measures. The evaluation of the MR dampers includes subjecting them to varying levels of displacement, 5 to 15 mm, and current, 1 to 3 A, at a frequency of 0,2 Hz, subjected to cyclic loading. This project aims to compare the performance and effectiveness of the two damper configurations.

2 MR damper

The proposed device is a smart device used to dissipate vibrations in structures. This MR damper operates based on the principles of magnetorheology, a technology that involves the use of magnetizable particles in a fluid to alter its rheological properties in response to an applied magnetic field. MR dampers respond rapidly to changing external conditions, providing real-time adjustments to mitigate the effects of dynamic forces. This responsiveness is crucial to enhance the performance and safety of structures during seismic events. In this study, mild steel-grade ASTM A32 was used to fabricate the single- and multi-coil MR dampers. The ASTM A32 mild steel grade offers corrosion resistance, consistent properties, and good machinability. The objective of this study is to compare single- and multi-coil MR dampers subjected to cyclic loading.

2.1 Single-coil MR damper

A single-coil MR damper is an innovative device intended to mitigate vibrations in structures caused by earthquakes or other natural disasters. The damper includes a cylindrical casing with an outer diameter of 60 mm, inner diameter of 50 mm, and depth of 280 mm. The piston, which has a diameter of 25 mm and length of 130 mm, plays a crucial role in the semi-active

system. It is wound with a 0,711 mm copper wire (22 standard wore gauge (SWG)) with a resistance of 29 Ω and a total of 1462 coil turns, thereby enabling the modulation of magnetic properties. The cylindrical head, with outer and inner diameters of 80 and 26 mm, respectively, completes the enclosure.
The semi-active nature of the MR damper is achieved by incorporating two open-coil helical springs positioned at the top and bottom of the piston. These springs, at a height and diameter of 55 and 45 mm, respectively, contribute to the adaptive behaviour of the damper. The MR fluid within the device includes a dynamic element that responds to the magnetic fields generated by the copper wire wound on the piston. A schematic of a single-coil MR damper is show in Figure 1.

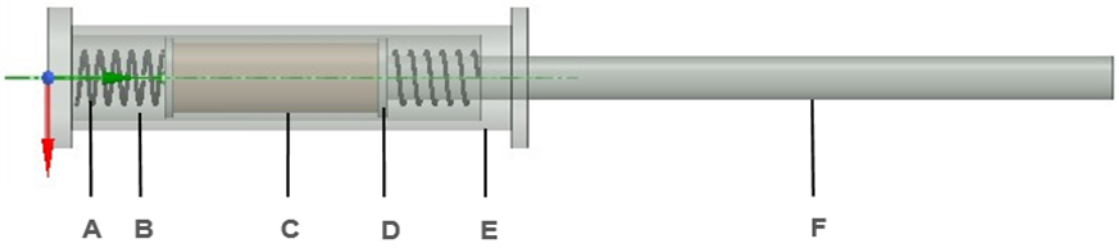

Figure 1. a) Spring, b) MR fluid, c) Copper coil, d) Piston, e) Cylinder casing, f) Piston rod

2.2 Multi-coil MR damper

In this study, a novel multi-coil MR damper is fabricated using a cylinder casing, cylinder head, multi-coil piston, and spring. The cylinder casing has an outer diameter, an inner diameter, and a depth of 60, 50, and 280 mm, respectively. The cylinder head comprises outer and inner diameters of 80 and 26 mm, respectively. The piston, with a length of 140 mm, features 10 coils and 11 piston teeth, each with a distance of 10 mm between them and a thickness of 5 mm, as shown in Figure 2.
The change in the shape of the piston results in an increase in the damping force compared to a single-coil piston. Each coil in the piston is wound with a 0,711-mm diameter copper wire 22 SWG for 137 turns. Two open-coil helical springs are used to make the damper semi-active, with an outside diameter of 45 mm, a pitch distance of 3 mm, and a height of 55 mm, and they are placed at the top and bottom of the multi-coil piston. Finally, MR fluid is filled in the cylinder casing. An annular gap of 1 mm between the piston and inner cylinder allows MR fluid to flow during vibration, providing the maximum damping force.

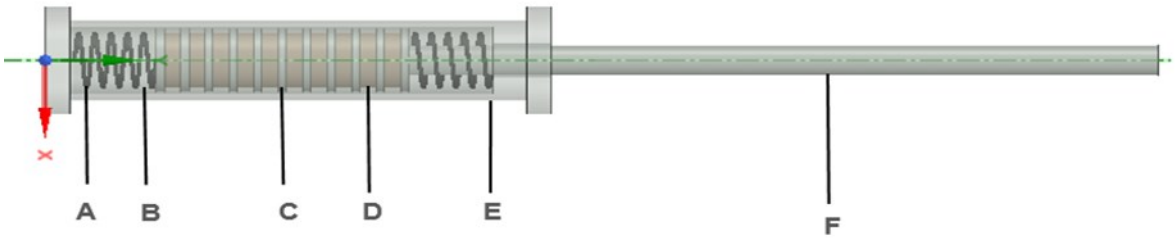

Figure 2. a) Spring, b) MR Fluid, c) Piston tooth, d) Copper coil, e) Cylinder casing, f) Piston rod

The integration of multiple coils, strategic piston design, and incorporation of springs render this multi-coil MR damper a sophisticated and efficient solution for dynamic damping in various applications.

3 MR fluid

MR Fluid is a smart liquid comprising a mixture of synthetic oils and magnetic particles. When exposed to a magnetic field, the particles align themselves within the liquid, resulting in changes in viscosity, yield stress, and magnetic susceptibility. The high susceptibility of the fluid enables precise control. Through experimentation, a combination of CI and synthetic oil was determined to be the most effective without the addition of surfactants. The spherical shape of the CI allows for good suspension within the fluid, and its high saturation magnetisation contributes to its effectiveness. To synthesise the fluid, grade R CI is mixed with the carrier fluid and stirred for 8 h at room temperature. The final mixture contains 50 % CI and 50 % carrier fluid. This proposed MRF 50 exhibits a maximum yield stress of approximately 93,34 kPa and viscosity of 0,28 Pa s [16]. The proposed MR fluid is shown in Figure 3.

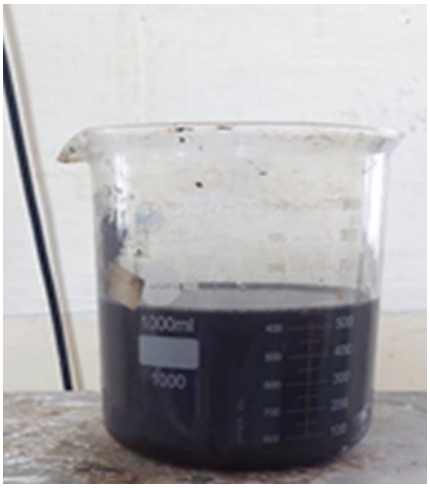

Figure 3. Proposed MR fluid

4 Numerical simulation of MR damper

To compare the performances of the single- and multi-coil MR dampers, the magnetic flux exerted by the dampers is studied. The MR damper is simulated using FEMM software, and its performance is tested by optimising the damper with different current inputs, from 1 to 3 A, in the coil.

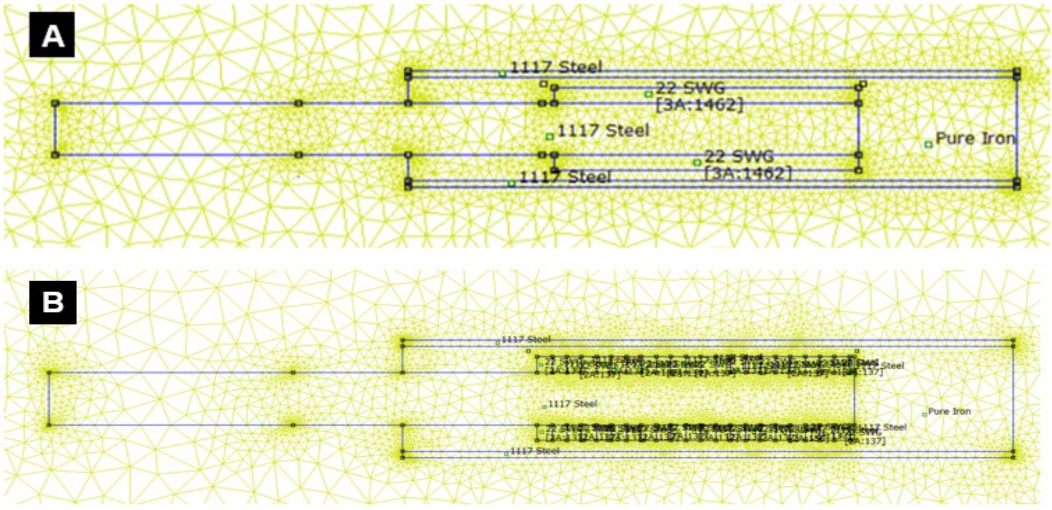

Figure 4. a) Meshing in single-coil MR damper, b) Meshing in multi-coil MR damper

Both the single- and multi-coil MR dampers are made of mild steel, which has low carbon and high manganese contents. For single- and multi-coil MR dampers, a 22SWG copper wire with a diameter of 0,8 mm is used. The total number of turns in the single-coil piston is approximately 1462. The multi-coil piston comprises 10 coils and 11 piston poles, and each toothing region has 137 turns of 22SWG copper coil. The meshing processes in single- and multi-coil MR dampers and the accurate results obtained from the simulation are shown in Figure 4.

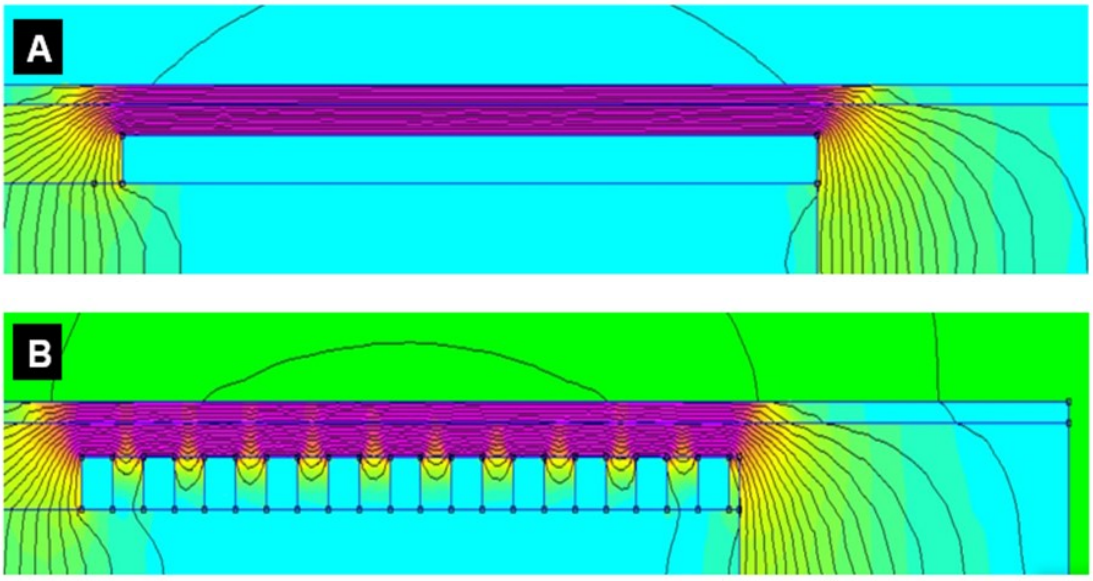

Figure 5. a) Flow of magnetic-flux lines in single-coil MR damper; b) Flow of magnetic-flux lines in multi-coil MR damper

The flow of the magnetic-flux lines across the annular gap in both the single- and multi-coil MR dampers is shown in Figure 5.

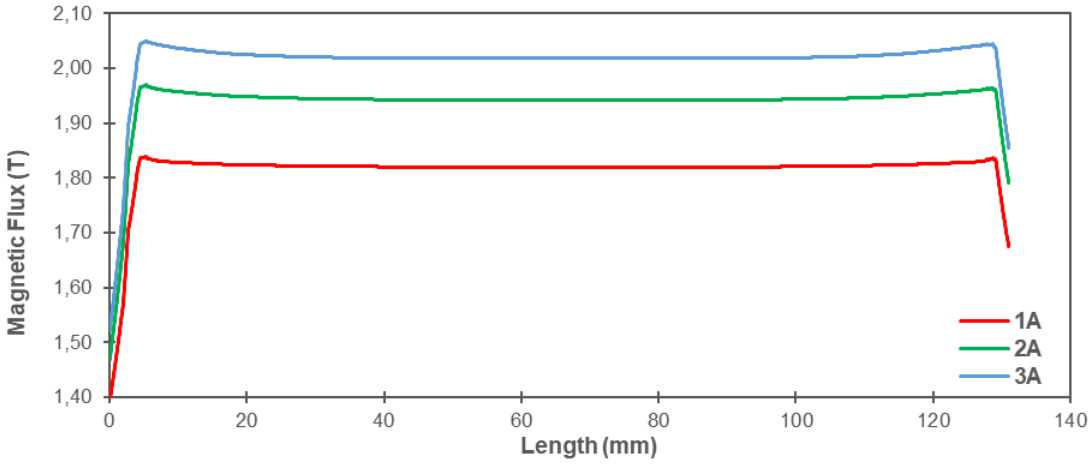

Figure 6. Magnetic flux in single-coil MR damper

These flux lines emerge from the coil and flow along the cylinder in the direction of the magnetic field. The intensity of the magnetic-flux lines is closer to the coil, leading to an apparent increase in the magnetic-field strength at the centre of the piston.

Figures 6 and 7 illustrate the differences in the flow of the magnetic-flux lines for the single- and multi-coil MR dampers with increasing input currents, from 1 to 3 A. The figures depict the magnetic-flux distribution along the annular gap between the piston and cylinder casing. As

the current increases, the density of the magnetic-flux lines also increases. A significant decrease is observed in Figure 7. This is because the piston poles do not create a magnetic flux. For the single-coil MR damper, the average magnetic-flux values are 1,81 T for 1 A, 1,94 T for 2 A, and 2,01 T for 3 A, and for the multi-coil MR damper, the averages are 1,9 T for 1 A, 2,02 T for 2 A, and 2,15 T for 3 A.

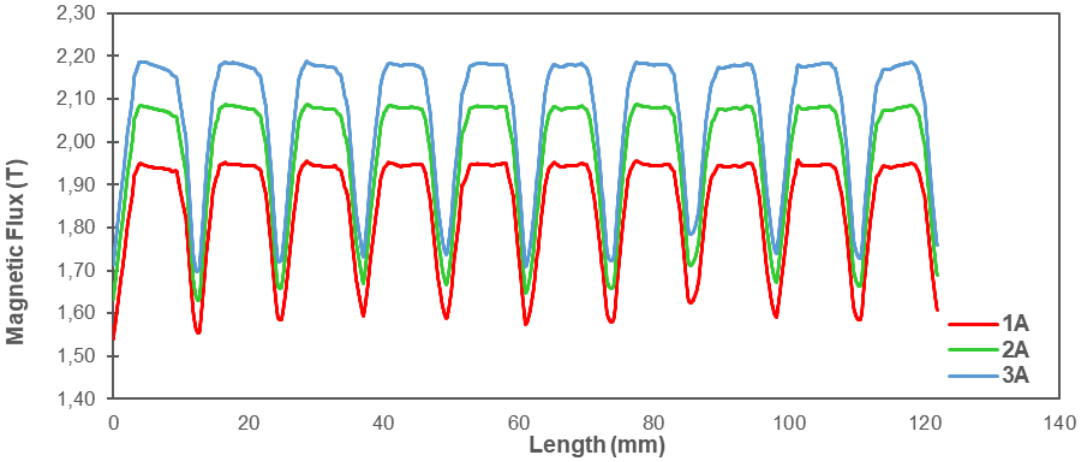

Figure 7. Magnetic flux in multi-coil MR damper

5 Experimental investigation

The performance of the damper can be determined by applying cyclic loading to MR dampers using the MTS universal testing machine (UTM) at the Karunya Institute of Technology and Sciences, Coimbatore. In the test, the frequency was maintained at 0,2 Hz, and currents of 0, 1, 2, and 3 A were applied. Amplitudes ranging from 5 to 15 mm were used. At a frequency of 0,2 Hz, a sinusoidal loading pattern would have had one complete cycle (from one peak to the next or from one trough to the next) every 5 s. Figure 8 shows the sinusoidal loading pattern for displacements ranging from 5 to 15 mm at a frequency of 0,2 Hz. In the test, the frequency was kept constant at 0,2 Hz, and currents of 0, 1, 2, and 3 A were applied. The amplitude was varied from 5 to15 mm. Figure 9 illustrates cyclic-loading tests set up on single- and multi-coil MR dampers. The experimental setup includes a load cell, base plate, hydraulic actuator, and regulated DC power supply. The piston base is fixed to the UTM base plate using a fixture, and the piston rod is attached to the load cell. The current to the coil is supplied by a DC power supply. The UTM input is controlled using a computer-regulated hydraulic actuator.

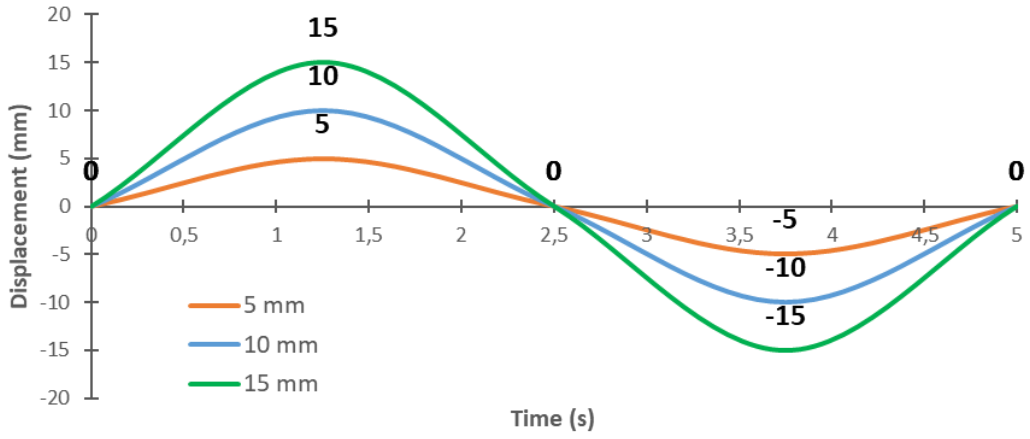

Figure 8. Cyclic-loading pattern subjected to MR damper

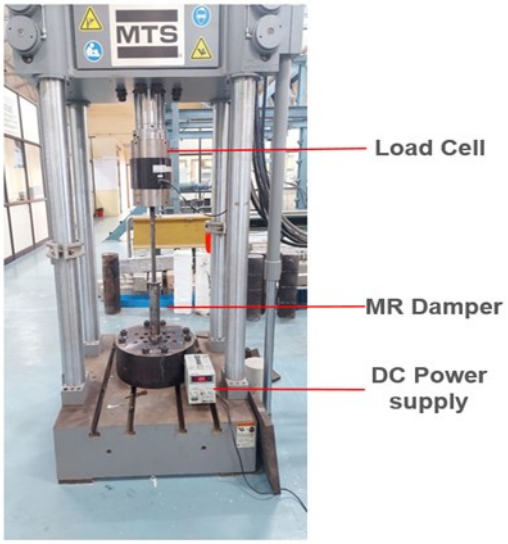

Figure 9. MR damper test setup

6 Results and discussion

The performance of single- and multi-coil MR dampers was evaluated under cyclic loading with varying displacements and current inputs. The graph shows the force versus displacement hysteresis behaviour. The graph is divided into four quadrants, where the first and second quadrants represent the compression phase and the third and fourth quadrants represent the tensile phase. The abscissa (x-axis) represents the load, and the ordinate (y-axis) represents the displacement.

As it is visible on Figure 10, the single-coil MR damper with a displacement of 5 mm, the maximum damping forces are 603,61, 794,45, 912,39, and 1072,58 N for applied currents of 0, 1, 2, and 3 A, respectively. Similarly, for a 10 mm amplitude in the single-coil MR damper, the maximum damping forces are 817,72, 1222,86, and 1444,33 N for applied currents of 0, 1, 2, and 3 A, respectively. Moreover, for a 15 mm amplitude, the maximum damping-force values are 1263,77, 1489,30, 1668,01, and 1868,83 N for the respective applied currents of 0, 1, 2, and 3 A, respectively.

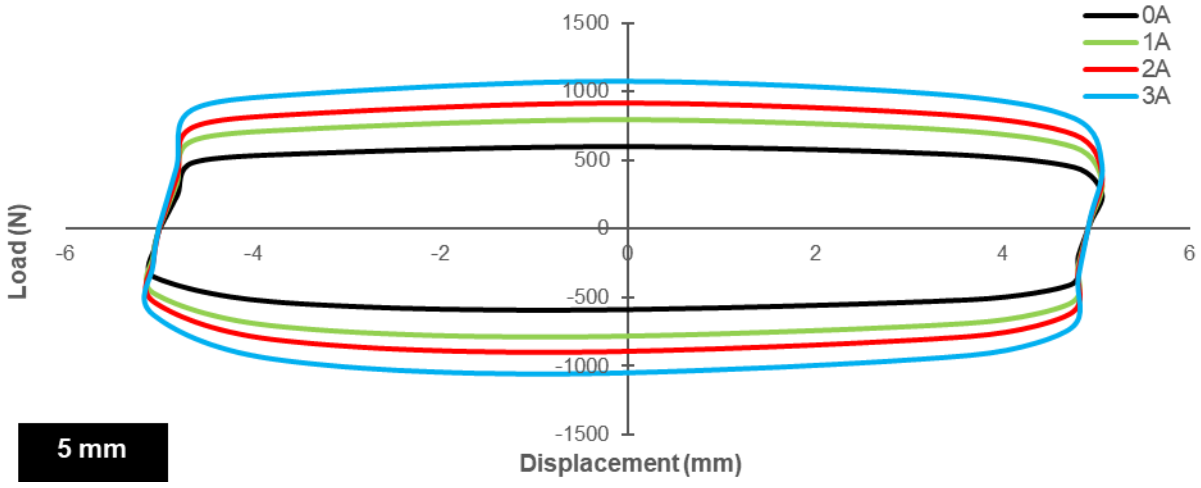

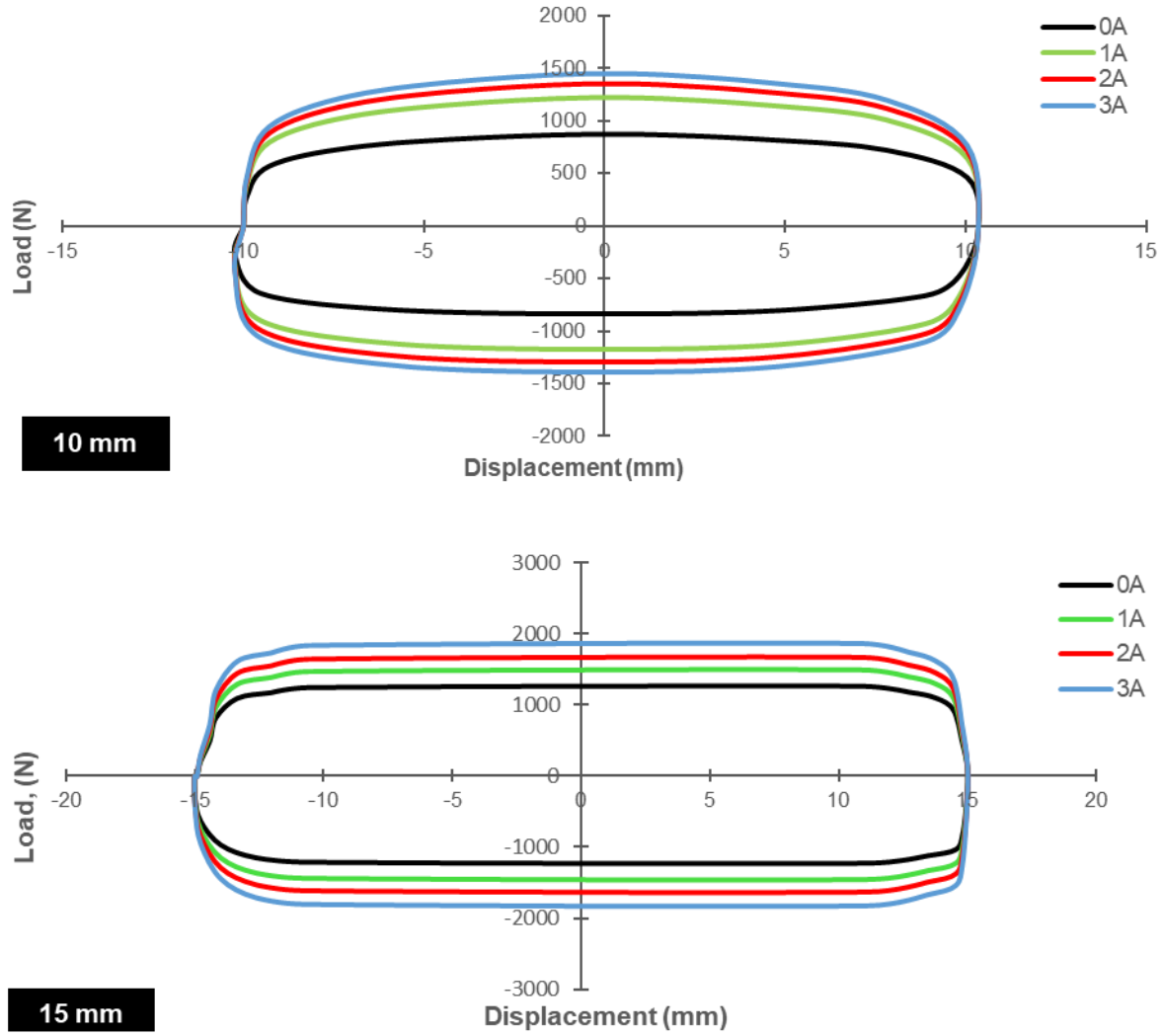

Figure 10. Force versus displacement for single-coil MR damper

In the case of the multi-coil MR damper (Figure 11) with a 5 mm displacement, the applied currents of 0, 1, 2, and 3 A result in maximum damping forces of 923,52, 1183,06, 1331,5, and 1511,05 N, respectively. Similarly, with a 10 mm amplitude in the multi-coil MR damper, the damping forces peak at 1240,32, 1492,42, 1579,40, and 1765,95 N for applied currents of 0, 1, 2, and 3 A, respectively. Furthermore, with a 15 mm amplitude, the maximum damping-force values are 1505,92, 2116,12, 2457,66, and 2628,29 N corresponding to applied currents of 0, 1, 2, and 3 A, respectively.

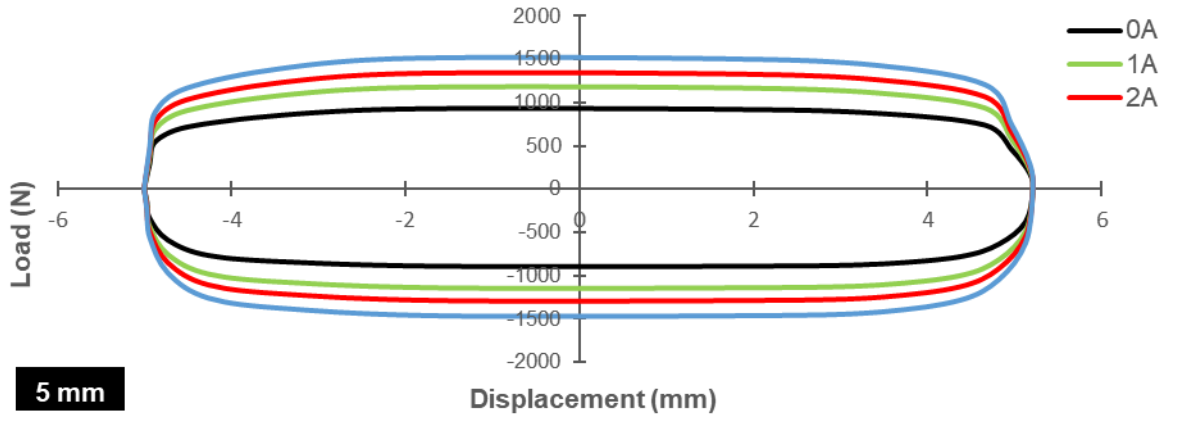

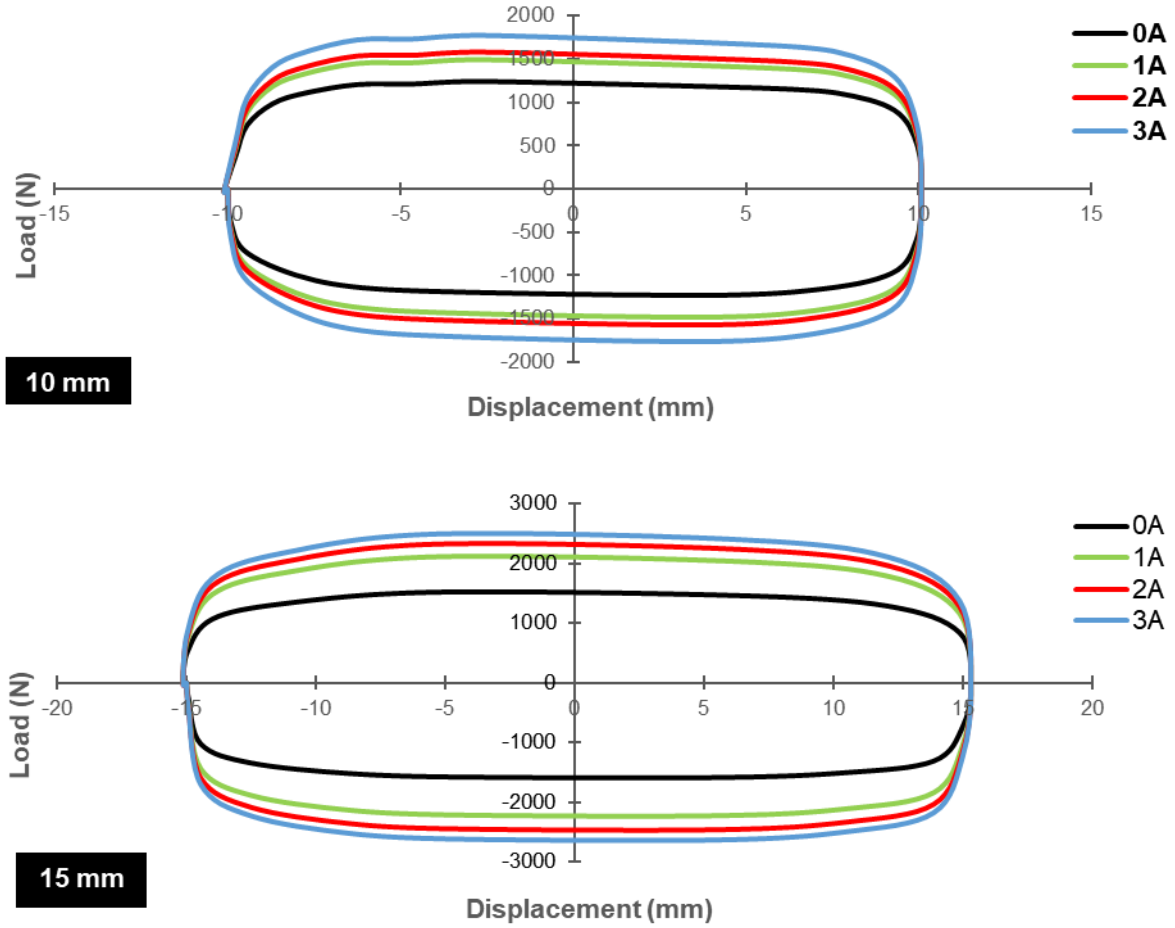

Figure 11. Force versus displacement of multi-coil MR damper

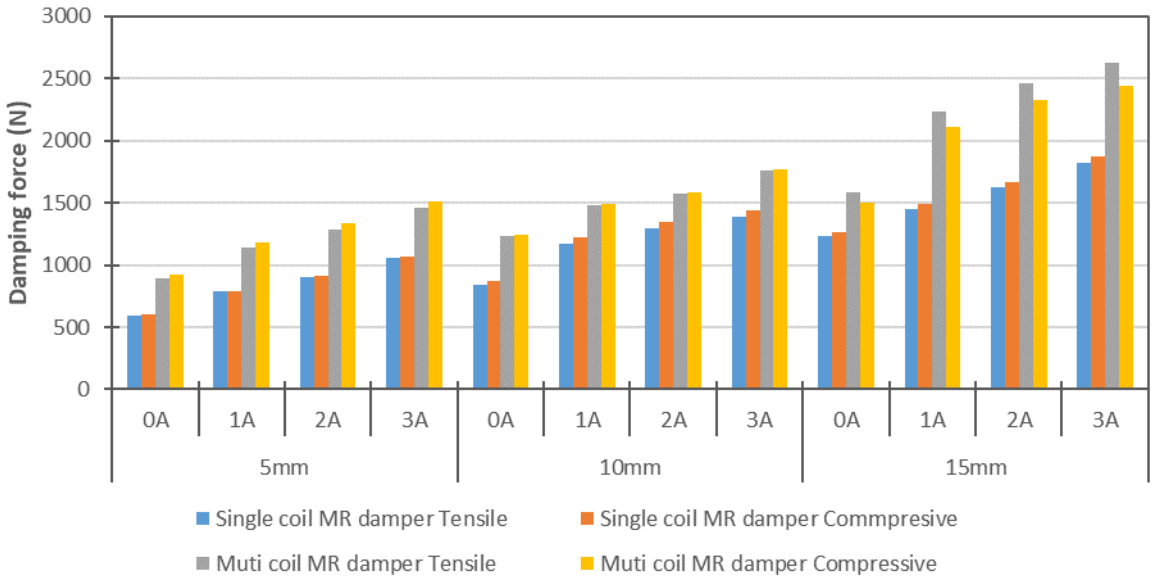

Figure 12. Comparison of damping forces between Single and Multi-coil dampers

Many significant trends and insights are revealed by comparing the damping forces of single-coil and multi-coil MR dampers. Multi-coil dampers consistently show larger damping forces

than their single-coil counterparts under all measured scenarios as depicted in Figure 12. This pattern is consistent for both compressive and tensile modes, demonstrating the enhanced ability of multi-coil designs to resist motion. Notably, for both types of dampers, the compressive forces are typically greater than the tensile forces. There is a proportionate link between current intensity and damping capabilities, as evidenced by the fact that the damping force also increases with the provided current. Higher currents cause a noticeable increase in damping force at all three displacement levels (5mm, 10mm, and 15mm), highlighting the usefulness of current management in adjusting damper performance. Moreover, there is a corresponding increase in damping force when the displacement is increased from 5mm to 15mm, highlighting the reliance of damping performance on the amplitude of motion. Overall, the data shows that multi-coil MR dampers are a better option for applications requiring stable and tunable damping solutions because they provide better damping performance, particularly in compressive mode and at greater currents and displacements.

7 Conclusions

In conclusion, the performance and behaviour of single- and multi-coil MR dampers under cyclic loading for various currents were studied. The results show that the multi-coil piston exerts a greater magnetic flux than the single-coil piston.

- The maximum forces exerted by single- and multi-coil MR dampers under cyclic loading were 1868,83 N and 2628,29 N at 15 mm displacement, respectively. The 30,58 % increment from the single-coil to multi-coil MR damper was attributed to the higher density of the magnetic-flux lines in the multi-coil configuration compared to the single-coil MR damper. The input current was directly proportional to the damping force.
- The MR fluid volume in the single-coil MR damper was 409,76 ml, and 352,92 ml in the multi-coil MR damper, indicating a reduction of 16 % in the volume of the MR fluid. This reduction reduces the cost of the MR damper when it is fabricated with a large loading capacity.
- Numerical simulations were conducted using FEMM to examine the flow of the magnetic flux in the damper. The experimental results showed that the maximum magnetic-flux values for the single- and multi-coil MR dampers were 2,01 and 2,15 T, respectively, for an applied current of 3 A. A 6,9 % increment in the magnetic-flux lines was observed in the multi-coil MR damper when compared to the single-coil MR damper.
- In the future, the damper should be placed diagonally in the RC frame. The damper performance can be studied when the frame is subjected to cyclic loading and real-time earthquake loading.

Acknowledgement

The authors express their gratitude to the Centre for Research & Consultancy at Hindustan Institute of Technology and Science in Padur, Chennai for providing the seed grant (SEED/CRC/HITS/2022-23/005).

References

[1] Cruze, D. et al. Seismic Mitigation of Building Frames using Magnetorheological Damper. *International Journal of Engineering*, 2019, 32 (11), pp. 1543-1547. https://doi.org/10.5829/ije.2019.32.11b.05

[2] Cruze, D. et al. Development of a Multiple Coil Magneto-Rheological Smart Damper to Improve the Seismic Resilience of Building Structures. *The Open Civil Engineering Journal*, 2020, 14. https://doi.org/10.2174/1874149502014010078

[3] Ratna, K. S. et al. Analytical Investigation of MR Damper for Vibration Control: A Review. *Journal of Applied Engineering Sciences*, 2021, 11 (1), pp. 49-52. https://doi.org/10.2478/jaes-2021-0007

[4] Desai, R. M. et al. Evaluation of a commercial MR damper for application in semi-active suspension. *SN Applied Sciences*, 2019, 1, 993. https://doi.org/10.1007/s42452-019-1026-y
[5] Kori, J. G.; Jangid, R. S. Semi-active MR dampers for seismic control of structures. *Bulletin of the New Zealand Society for Earthquake Engineering*, 2009, 42 (3), pp. 157-166. https://doi.org/10.5459/bnzsee.42.3.157-166
[6] Olivier, M.; Sohn, J. W. Design and geometric parameter optimization of hybrid magnetorheological fluid damper. *Journal of Mechanical Science and Technology*, 2020, 34, pp. 2953-2960. https://doi.org/10.1007/s12206-020-0627-0
[7] Cruze, D. et al. Seismic Performance Evaluation of a Recently Developed Magnetorheological Damper: Experimental Investigation. *Practice Periodical on Structural Design and Construction*, 2021, 26 (1), 04020061. https://doi.org/10.1061/(ASCE)SC.1943-5576.0000544
[8] Wang, M.; Chen, Z.; Wereley, N. M. Magnetorheological damper design to improve vibration mitigation under a volume constraint. *Smart Materials and Structures*, 2019 28 (11), 114003. https://doi.org/10.1088/1361-665x/ab4704
[9] Bharathi Priya, C.; Gopalakrishnan, N. Experimental investigations of the effect of temperature on the characteristics of MR damper. In: *Recent Advances in Structural Engineering, Volume 2: Select Proceedings of SEC 2016*, Rao, A.; Ramanjaneyulu, K. (eds.). Springer, Singapore; 2018, pp. 435-443. https://doi.org/10.1007/978-981-13-0365-4_37
[10] Heo, G. et al. Mitigate seismic response of three-span bridge using MR damping system. In: *Experimental Vibration Analysis for Civil Structures: Testing, Sensing, Monitoring, and Control 7*, Conte, J. et al. (eds.). Springer, Cham., 2017, pp. 547-556. https://doi.org/10.1007/978-3-319-67443-8_47
[11] Patel, J. D.; Patel, D. Design optimization of squeeze mode magnetorheological damper. *Applied Mechanics and Materials*, 2018, 877, pp. 391-396. https://doi.org/10.4028/www.scientific.net/AMM.877.391
[12] Yazid, I. I. M. et al. Design of magnetorheological damper with a combination of shear and squeeze modes. *Materials & Design (1980-2015)*, 2014, 54, pp. 87-95. https://doi.org/10.1016/j.matdes.2013.07.090
[13] Mohd Yamin, A. H.; Ab Talib, M. H.; Mat Darus, I. Z.; Mohd Nor, N. S. Magneto-rheological (MR) damper – parametric modelling and experimental validation for lord RD 8040-1. *Jurnal Teknologi*, 2022, 84 (2), pp. 27-34. http://dx.doi.org/10.11113/jurnalteknologi.v84.16611
[14] Aggümüş, H.; Güçlü, R. Hybrid experimental investigation of MR damper controlled tuned mass damper used for structures under earthquakes. *Journal of Soft Computing and Artificial Intelligence*, 2022, 3 (1), pp. 28-33. https://doi.org/10.55195/jscai.1122514
[15] Fu, W. et al. Experimental investigation of a base isolation system incorporating MR dampers with the high-order single step control algorithm. *Applied Sciences*, 2017, 7 (4), 344. https://doi.org/10.3390/app7040344
[16] Cruze, D. Study on Magnatec oil-based MR fluid and its damping efficiency using MR damper with various annular gap configurations. *Energy, Ecology and Environment*, 2021,6, pp. 44-54. https://doi.org/10.1007/s40974-020-00170-6
[17] Utami, D. et al. Material Characterization of a Magnetorheological Fluid Subjected to Long-Term Operation in Damper. *Materials*, 2018, 11 (11), 2195. https://doi.org/10.3390/ma11112195
[18] Wen, M. et al. Characterization of magnetorheological fluids based on capillary magneto-rheometer. *Frontiers in Materials*, 2022, 9, 1034127. https://doi.org/10.3389/fmats.2022.1034127
[19] Emagbetere, E.; Zuokumor, K. C. Artificial Neural Network for Modelling the Performance of Carbonyl-Iron Particle-Paraffin Oil-Based Magneto-Rheological Fluid. *Nigerian Research Journal of Engineering and Environmental Sciences*, 2022, 7 (1), pp. 156-167. http://doi.org/10.5281/zenodo.6722564

[20] Cruze, D. et al. Magnetorheological Fluid with Nano Fe3O4 for Performance Enhancement of MR Damper for Seismic Resistance of Steel Structures. *Key Engineering Materials*, 2018, 763, pp. 975-982. https://doi.org/10.4028/www.scientific.net/kem.763.975

[21] Abdalaziz, M.; Vatandoost, H.; Sedaghati, R.; Rakheja, S. Development and experimental characterization of a large-capacity magnetorheological damper with annular-radial gap. *Smart Materials and Structures*, 2022, 31 (11), 115021. https://doi.org/10.1088/1361-665x/ac9a16

[22] Devikiran, P.; Puneet, N. P.; Hegale, A.; Kumar, H. Design and development of MR damper for two wheeler application and Kwok model parameters tuning for designed damper. *Proceedings of the Institution of Mechanical Engineers, Part D: Journal of Automobile Engineering*, 2022, 236 (7), pp. 1595-1606. https://doi.org/10.1177/09544070211036317

[23] Jiang, M. et al. Multi-objective optimization design for a magnetorheological damper. *Journal of Intelligent Material Systems and Structures*, 2022, 33 (1), pp. 33-45. https://doi.org/10.1177/1045389x211006907

[24] Zhang, Y.; Guo, J.; Yang, J.; Li, X. Recent Structural Developments and Applications of Magnetorheological Dampers (MRD): A Review. *Magnetochemistry*, 2023, 9 (4), 90. https://doi.org/10.3390/magnetochemistry9040090

[25] Tharehalli Mata, G.; Mokenapalli, V.; Krishna, H. Performance analysis of MR damper based semi-active suspension system using optimally tuned controllers. *Proceedings of the Institution of Mechanical Engineers, Part D: Journal of Automobile Engineering*, 2021, 235 (10-11), pp. 2871-2884. https://doi.org/10.1177/09544070211004467